Photochemical & Photobiological Sciences

PAPER

View Article Online
View Journal

Cite this: DOI: 10.1039/c8pp00307f

Automated on-line monitoring of the TiO_2-based photocatalytic degradation of dimethyl phthalate and diethyl phthalate†

Daniel Salazar-Beltrán,[a,b] Laura Hinojosa-Reyes, [a] Fernando Maya-Alejandro, [b] Gemma Turnes-Palomino, [b] Carlos Palomino-Cabello, [b] Aracely Hernández-Ramírez [a] and Jorge Luis Guzmán-Mar *[a]

A fully automated on-line system for monitoring the TiO_2-based photocatalytic degradation of dimethyl phthalate (DMP) and diethyl phthalate (DEP) using sequential injection analysis (SIA) coupled to liquid chromatography (LC) with UV detection was proposed. The effects of the type of catalyst (sol–gel, Degussa P25 and Hombikat), the amount of catalyst (0.5, 1.0 and 1.5 g L^{-1}), and the solution pH (4, 7 and 10) were evaluated through a three-level fractional factorial design (FFD) to verify the influence of the factors on the response variable (degradation efficiency, %). As a result of FFD evaluation, the main factor that influences the process is the type of catalyst. Degradation percentages close to 100% under UV-vis radiation were reached using the two commercial TiO_2 materials, which present mixed phases (anatase/rutile), Degussa P25 (82%/18%) and Hombikat (76%/24%). 60% degradation was obtained using the laboratory-made pure anatase crystalline TiO_2 phase. The pH and amount of catalyst showed minimum significant effect on the degradation efficiencies of DMP and DEP. Greater degradation efficiency was achieved using Degussa P25 at pH 10 with 1.5 g L^{-1} catalyst dosage. Under these conditions, complete degradation and 92% mineralization were achieved after 300 min of reaction. Additionally, a drastic decrease in the concentration of BOD_5 and COD was observed, which results in significant enhancement of their biodegradability obtaining a BOD_5/COD index of 0.66 after the photocatalytic treatment. The main intermediate products found were dimethyl 4-hydroxyphthalate, 4-hydroxy-diethyl phthalate, phthalic acid and phthalic anhydride indicating that the photocatalytic degradation pathway involved the hydrolysis reaction of the aliphatic chain and hydroxylation of the aromatic ring, obtaining products with lower toxicity than the initial molecules.

Received 13th July 2018,
Accepted 10th September 2018

DOI: 10.1039/c8pp00307f

rsc.li/pps

1. Introduction

Phthalic acid esters (PAEs) have been classified as priority hazardous substances due to their risk to human health. PAEs have been widely used as additives in plastic or polymeric materials to improve their flexibility, transparency, and durability.[1–3] Today, millions of tons of PAEs are produced all over the world annually.[4–6] These poorly biodegradable PAEs are not chemically bound to polymers and can easily reach the soil and aquatic systems.[7] The main concern related to PAEs exposure is their effect on humans and wildlife reproduction,[8,9] causing damage to the endocrine system and carcinogenic effects.[10–12] Due to the risk to human health and the environment, certain PAEs including dimethyl phthalate (DMP) and diethyl phthalate (DEP) have been identified as priority hazardous substances by the European Union (EU).[13,14]

Most commonly, these short chained esters are detected in environmental samples,[5,15] including rivers, lakes and groundwater. Different physical and chemical processes like adsorption with activated carbon, chitosan, or activated sludge have been described for the removal of PAEs from water.[5,16,17] However, the pollutants are only concentrated onto adsorbent materials. Thus, it is necessary to identify appropriate treatment technologies such as advanced oxidation processes (AOPs), which involve the generation and use of transient species of high oxidizing power, mainly the hydroxyl radical (•OH). Within these processes, heterogeneous photocatalysis has been proposed in recent years as an interesting alternative

[a]Universidad Autónoma de Nuevo León, Facultad de Ciencias Químicas, San Nicolás de los Garzas, Nuevo León, C.P. 66455, Mexico.
E-mail: jorge.guzmamr@uanl.edu.mx
[b]University of the Balearic Islands, Department of Chemistry, Cra. de Valldemossa Km 7.5, Palma de Mallorca, E-07122, Spain

†Electronic supplementary information (ESI) available. See DOI: 10.1039/c8pp00307f

for PAEs oxidation; nevertheless, much work has been done on the degradation of single pollutants.[18–20] Titanium dioxide (TiO_2) is known to be an excellent photocatalyst because it is photostable, reusable, inexpensive, nontoxic and easily available.[21–23] Anatase and rutile are the two principal catalytic phases of TiO_2. Anatase is generally regarded as the most photochemically active phase of TiO_2, presumably due to the combined effect of lower rates of recombination and higher surface adsorptive capacity.[24] Compared with pure phase TiO_2 materials, mixed-phase TiO_2 can exhibit higher photocatalytic activity, which could be attributed to the effective interparticle charge transfer that promotes charge separation and enhances photoactivity and photoefficiency.[25,26]

Degradation studies are primarily based on batch treatments, and proper analytical control is often time-consuming due to the collection of a considerable number of samples at fixed times during the evolution of the photocatalytic reaction. In this sense, sequential injection analysis (SIA) has proved to be a suitable system for on-line analysis because of its high sampling frequency, simplicity of automation, minimal sample and reagent consumption, and little sample manipulation.[27–29]

In this work, the application of heterogeneous photocatalysis for the degradation of a binary mixture of DMP and DEP under UV-Vis radiation was investigated. The on-line and real-time monitoring of pollutant degradation was carried out using an SIA system equipped with a photoreactor, which is coupled to a high performance liquid chromatography instrument. The effect of catalyst type, catalyst dosage and solution pH was studied comparing the photocatalytic activity of three different TiO_2-based materials. Under the selected degradation conditions, complementary tests were performed, following the mineralization and the biodegradability index. Finally, gas chromatography coupled to mass spectrometry (GC-MS) was used to identify the degradation intermediates and by-products. Based on the detected intermediates, degradation pathways of DMP and DEP were proposed in the TiO_2 photocatalytic system. To the best of the authors' knowledge, the photocatalytic oxidation of a mixture of PAEs has not been studied yet under the above-mentioned conditions.

2. Experimental

2.1. Implementation of an automated SIA photocatalytic reactor

The SIA system (Fig. 1) for the on-line monitoring of the photocatalytic degradation of DMP and DEP was composed of a syringe pump (SIA) and an 8-port multi-position selection valve. The SIA system was coupled to the photocatalytic reactor (a 250 mL Pyrex glass reactor and a UV-visible metal halide Philips lamp 25 W, polychromatic radiation from 300 to 700 nm, 563 W m^{-2}) and to a filtration unit through the multi-position selection valve. The lamp was positioned at a distance of 5 cm above the reactor. Aqueous DMP and DEP mixture solution with an initial concentration of 5 mg L^{-1} for each compound was prepared at different pH values (4, 7 and 10) adjusted using diluted aqueous solutions of HCl and NaOH. The dosage of the catalyst was between 0.5 and 1.5 g L^{-1}. Catalyst dispersions were equilibrated in the dark for 1 h prior to irradiation. At regular time intervals (30 min), 2 mL of the sample were automatically loaded from the reactor and filtered through a 0.45 μm Nylon filter to remove the photocatalyst. The concentrations of DMP and DEP were analyzed using a Jasco high performance liquid chromatography (HPLC) system with a C18 Column (Phenomenex Kinetex, 5 mm × 4.6 mm i.d.) and a UV-Vis diode array detector (MD-4017) at 230 nm. Isocratic elution with acetonitrile/water (55 : 45, v/v) mobile

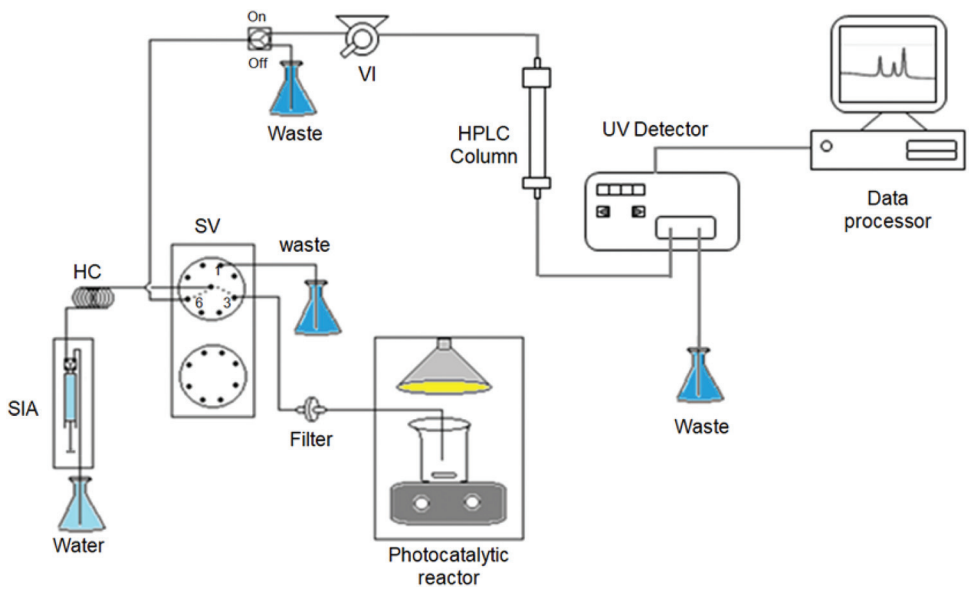

Fig. 1 A schematic depiction of the SIA system used for the on-line monitoring of DMP and DEP during the photocatalytic reaction.

phase at a flow rate of 1 mL min^{-1} and an injection volume of 20 μL was used. The calibration curves were elaborated from seven concentration standards from 0.1 and 10 mg L^{-1}, and the limits of detection were 0.01 and 0.02 mg L^{-1} for DMP and DEP, respectively.

2.2. Characterization of TiO_2-based photocatalysts

Catalyst surface area and porosity were determined from the nitrogen adsorption measurements at 77 K. The crystalline phase composition and the average crystallite size were studied using X-ray diffraction (XRD). The morphology of the catalysts was analyzed using scanning electron microscopy (SEM). Diffuse reflectance UV-Vis spectroscopy was used to obtain the band gap energy. The isoelectric point was determined using a Zeta-Meter apparatus. Detailed information is described in the ESI.†

2.3. Statistical analysis

A three-level fractional factorial design (FFD) with three replicates at the central point was used to investigate the effect of the process variables as well as to identify the best conditions for the photocatalytic process. Three independent variables were type of catalyst (TC), dosage of catalyst (CC), and solution pH (pH). The degradation percentages of DMP and DEP at 150 min reaction time were the output response variables.

The significance of the effects of each variable was evaluated with analysis of variance (ANOVA) using the statistical software STATISTICA 10 (StatSoft, Inc. 2011). A *p*-value of less than 0.05 was considered significant. To evaluate the statistical relationships among operating variables of the photocatalytic process and the responses (degradation percentages of DMP and DEP) was used a response surface methodology approach and desirability parameters.

2.4. Determination of total organic carbon (TOC) and the biodegradability index

A volume of 8 mL of the sample was taken from the reactor every 60 min. The samples were filtered through a 0.45 μm Nylon syringe filter to remove TiO_2 particles and acidified to pH 2 with 1 M HCl prior to analysis. The total organic carbon (TOC) concentration was measured using a Multi N/C 2100s analyzer (Analytik Jena AG Corporation).

For the analysis of the biological oxygen demand (BOD_5) and the chemical oxygen demand (COD), volumes of 25 mL of the sample were taken every hour during the photocatalytic degradation and prepared for their analysis on the same day. COD was determined using the closed reflux method (Method 5220 D) and the consumed oxygen was measured at 600 nm using a Hewlett-Packard 8452A UV-Vis spectrophotometer.[30] For the determination of BOD_5, a sensor system was used (VELP SCIENTIFICA).[30]

The BOD_5 and COD measurements were used to calculate the biodegradability index. There is a correlation between the BOD_5 and COD values under certain conditions.[31]

The BOD_5/COD ratio is usually greater than 0.5 for highly biodegradable samples, between 0.4 and 0.5 for moderately biodegradable samples, between 0.2 and 0.4 for samples with low biodegradability, and less than 0.2 for non-biodegradable samples.[32]

2.5. Identification of degradation intermediates and by-products

To determine the intermediate products from the DMP and DEP photocatalytic reaction, solid-phase extraction (SPE) with C18 25 mm 3 M Empore extraction disks was used.[33] The extraction disk was conditioned with 10 mL of a dichloromethane and ethyl acetate mixture (1 : 1), 10 mL of methanol, and 10 mL of ultrapure water. Then, the sample was percolated through the disk with a flow rate of 5 mL min^{-1} under vacuum. The compounds trapped in the disk were collected using 5 × 4 mL of dichloromethane/ethyl acetate (1 : 1). The collected fractions were evaporated under a gentle stream of nitrogen to dryness, reconstituted in 100 μL of the solvent mixture, and 1 μL was injected into the GC-MS instrument in a splitless mode. A GC-MS system (5979 inert XL mass selective, Agilent Technologies) equipped with an Agilent HP-5 ms capillary column (30 m × 0.25 mm i.d.) was used with the following chromatographic conditions: injector temperature 220 °C, column temperature program 40 °C, 40–200 °C (5 °C min^{-1}), 200–210 °C (1 °C min^{-1}), 210–280 °C (20 °C min^{-1}) and 280 °C (3 min). Helium was used as the carrier gas at 1.5 mL min^{-1}. The interface was kept at 280 °C.[33]

The by-products of the degradation reaction were analyzed using ion exclusion chromatography (IEC). At regular time intervals (60 min), 1 mL of the sample was taken from the reactor and filtered through 0.45 μm Nylon syringe filters to remove TiO_2 particles. The degradation by-products were analyzed on a YL9100 HPLC system with an ion exclusion column (Aminex, 300 mm × 7.8 mm i.d.) equipped with a photodiode array detector (YL9160) at 200 nm. The mobile phase was 4 mM H_2SO_4 at a flow rate of 0.8 mL min^{-1} with an injection volume of 20 μL.

3. Results and discussion

3.1. Characterization of TiO_2-based photocatalysts

The characterization results of TiO_2-based materials are summarized in Table 1. The crystallinity and growth orientation of the TiO_2 materials were examined using XRD (Fig. S1†). The composition of the crystalline phase was determined with eqn (S1)† showing that Degussa P25 has 82% anatase and 18% rutile, while Hombikat has 76% anatase and 24% rutile (Table 1). The contents of crystalline phases were similar to those published by Karunakaran *et al.*[34]

The average crystallite sizes of the anatase phase were determined using eqn (S2),† obtaining values of 19.5, 20.7 and 20.7 nm for sol–gel, Degussa P25 and Hombikat, respectively, showing slightly higher values for the commercial TiO_2-based materials compared to that of the material prepared by the sol–gel method.

Table 1 Characteristics of TiO_2 based catalysts

Catalyst	Crystalline phase (%) (A: anatase, R: rutile)	Surface area ($m^2\ g^{-1}$)	Pore size (nm)	E_g (eV)	Isoelectric point
Sol–gel	100 (A)	49.2	8.0	3.0	6.1
Degussa P25	82 (A)/18 (R)	51.4	22.7	3.1	6.5
Hombikat	76 (A)/24 (R)	56.9	26.0	3.1	6.9

The surface areas and pore sizes were calculated by the BET method and BJH method, respectively, from the N_2 adsorption isotherms (Fig. S2†). Although the surface areas of the three materials were very similar (Table 1), the fact that commercial materials show a 3-fold larger pore size than the synthesized material by the sol–gel method can be attributed to a pore blocking by a process of percolation in the sol–gel material (hysteresis loop type H2). A larger pore size can make these pores more accessible to PAE molecules, increasing the adsorption and degradation of the pollutant.[35,36]

From the diffuse reflectance UV-Vis absorption spectrum (Fig. S3†) and applying the Kubelka–Munk equation,[37] the band gap energy (E_g) of each catalyst was calculated. The E_g values of the materials (Table 1) were similar (3.0–3.1 eV), which means that these materials absorb energy that lies at the boundary between the UV and the visible region. The catalysts presented an isoelectric point between pH 6 and 7 (Fig. S4†), having the lowest value (6.1) for the TiO_2 synthesized by the sol–gel method, followed by Degussa P25 (6.5) and finally the Hombikat (6.9).

SEM images of the catalysts are shown in Fig. S5.† The three materials had a similar morphology based on the agglomeration of spherical particles with sizes close to 50 nm for the sol–gel TiO_2, lower than 50 nm for Degussa P25, and close to 100 nm for Hombikat. Particle size is an important parameter influencing catalytic activity; a high photocatalytic activity is associated with a smaller particle and crystallite size, due to the fact that a large number of active surface sites are available for adsorption, which increases the rate of interfacial charge transfer.[36,38]

3.2. Implementation of the automated SIA photocatalytic reactor

The SIA system allowed all solutions to be handled during the monitoring of the PAE degradation in a fully automated mode. Ten aliquots were collected during the photocatalytic reaction and analyzed in triplicate. Aliquots of 2 mL of the PAEs/TiO_2 dispersion were collected every 30 min and analyzed after the removal of TiO_2 by on-line filtration. It was not necessary to replace the filter during the photocatalytic reaction. Any change in the peak shape and resolution, and backpressure problems in the system were observed using the same filter. On-line monitoring was compared with manual analysis showing a relative standard deviation of the peak area values of less than 3.9% in the case of the manual analysis and less than 1.6% in the case of the automated system, demonstrating the precision of the proposed automated procedure.

3.3. Significance of process variables and empirical model development for PAE photocatalytic degradation

The significance of the process variables in terms of linear and quadratic effects was assessed using the Pareto chart at a 95% confidence level (Fig. S6†). The type of catalyst (TC) considerably affected the degradation percentage of both PAEs followed by the quadratic term of TC. The variable dosage of catalyst (CC) and the pH of the solution by themselves had little positive influence on the degradation percentage of both compounds.

In the ANOVA performed for the regression model, R^2 values of 99.29 and 99.71 were obtained for DMP and DEP, respectively. These results indicated that the predicted and the experimental values were similar with an error less than 5%.

Response surface graphs were constructed in terms of desirability to define the best conditions for degradation of DMP and DEP (Fig. 2). Regarding the type of catalyst (Fig. 2A and B), it was observed that the degradation efficiency was higher using Degussa P25, reaching percentages greater than 60% for both compounds after 150 min of the reaction, followed by the Hombikat reaching percentages close to 55%, and finally the TiO_2 synthesized by the sol–gel method showed a lower degradation percentage (near to 25%). The photocatalytic activity of TiO_2 depends on the surface and structural properties that include the crystalline composition, surface area, particle size distribution, porosity and band gap energy. The greater photocatalytic efficiency in the degradation of DMP and DEP using Degussa P25 and Hombikat catalysts may be due to the fact that these materials present a mixture of anatase and rutile crystalline phases and have a larger pore size, enhancing the accessibility of PAE molecules, in comparison with the one synthesized by the sol–gel method with only the anatase phase and considerably smaller pore size. Studies related to the photocatalytic activity of mixed phases of TiO_2 propose that the transfer of electrons from the anatase phase to an electron trap of the rutile phase of lower energy serves to reduce the recombination rate of the electron–hole pairs in the anatase phase and improve the photoactivity and photoefficiency of TiO_2-based catalysts. Moreover, the rutile phase helps by changing the photoresponse of the anatase phase to the visible region in mixed phase materials.[24,26] Among the commercial catalysts, the higher degradation percentages of DMP and DEP were obtained when using Degussa P25, which may be due to its phase composition (anatase–rutile ratio), while Hombikat presented a higher percentage of the rutile phase that may favor the recombination of electron–hole pairs.[24] Muneer *et al.* compared the performance of the catalysts Degussa P25 and

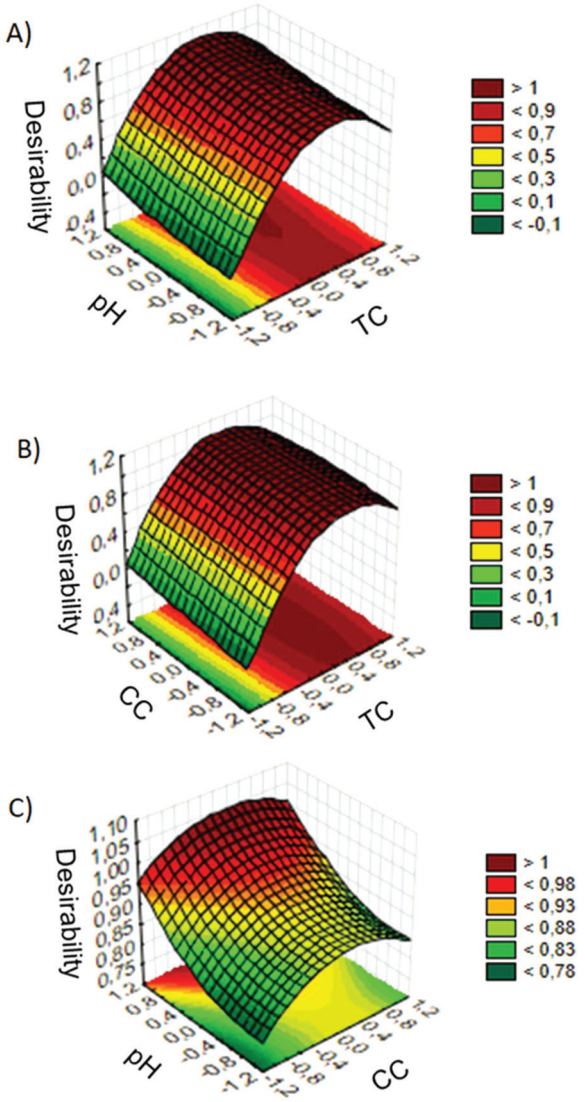

Fig. 2 Response surface of the desirability function for the degradation of DMP and DEP showing the mutual effect of the factors: A) pH and TC; B) CC and TC; and C) pH and CC.

Hombikat for DEP degradation, concluding that both materials exhibited a similar behavior in photonic efficiency; nevertheless, a higher degradation percentage was obtained when using Degussa P25.[39]

The effect of the catalyst dosage was investigated (Fig. 2B and C). Different catalyst loads were evaluated (from 0.5 to 1.5 g L^{-1}). The amount of catalyst in batch photoreactors is commonly described between 0.2 and 2.5 g L^{-1}. This limit depends on the geometry and working conditions of the photoreactor and corresponds to the maximum amount of TiO_2 in which all the exposed surface is fully irradiated. Exceeding this maximum concentration of the catalyst, a masking effect of the photosensitive surface occurs due to the excess of particles.[40–42] The degradation efficiency was enhanced by increasing the catalyst amount up to 1.5 g L^{-1}. The increase in the degradation efficiency of DMP and DEP was due to the increase in the total surface area of the catalyst (active sites) available for the photocatalytic reaction. This result agrees with that reported by Xu *et al.*, who evaluated Degussa P25 to degrade butylbenzyl phthalate (BBP) by varying the catalyst concentration between 0.5 and 5 g L^{-1}, concluding that the efficiency in the degradation of BBP increased with larger amounts of TiO_2 up to 2.0 g L^{-1}.[43]

Finally, the effect of the pH on the degradation of DMP and DEP was evaluated (Fig. 2A and C). In heterogeneous photocatalysis systems, pH is one of the operating parameters that affects the surface charge of the catalyst.[40] The pH of the solution modifies the surface charge of the catalyst, while DMP and DEP are in the molecular form over the entire pH range, so, they do not exhibit electrostatic interactions with the catalyst surface.[44] The percentage of degradation increased with the increase in pH values for the three catalysts, reaching the highest degradation percentage at pH 10. In general, changes in pH may have a non-significant effect on the adsorption of PAEs on the TiO_2 surface, as well as on the photodegradative reactions that occur on the surface of the particles.[33] However, all three catalysts presented their highest degradation efficiency at pH 10; this could be due to the fact that at high initial pH, more hydroxide ions (OH^-) are present in the solution, promoting the formation of hydroxyl radicals ($^{\bullet}OH$), which are produced by the photooxidation of OH^- ions through the holes formed in the surface of TiO_2. Since the $^{\bullet}OH$ radicals are the main oxidizing species in the photocatalytic process, the degradation of DMP and DEP can be accelerated in an alkaline medium.[45]

The estimated parameters by the desirability profiles (Fig. S7†) indicated that maximum degradation percentage values of DMP and DEP were 82.7 and 81.3%, respectively, at 150 min of the reaction, obtained with 1.5 g L^{-1} of the catalyst Degussa P25 at pH 10.

The photocatalytic reaction was carried out under these experimental conditions and degradation percentages of 81.0 and 82.2% for DMP and DEP were obtained with an error less than 2.1%. Control tests such as adsorption and photolysis were performed under operating conditions described by the experimental design and compared with the obtained results. Fig. 3A–B show the complete degradation for DMP and DEP at 250 min reaction time through the photocatalytic process, and adsorption did not contribute (less than 2% for both compounds) to the degradation. The photodegradation of PAEs under UV-Vis radiation was almost negligible (approximately 5%), confirming the effectiveness of the photocatalytic process during the degradation of the phthalate mixture.

3.4. Determination of total organic carbon (TOC) and the biodegradability index

Likewise, under the same conditions, the mineralization of the contaminants was evaluated during the photocatalytic process and the results are presented in Fig. 3C. The efficiency of the TiO_2 P25-based photocatalysis was clearly observed, since 92% mineralization was reached after 300 min of reaction.

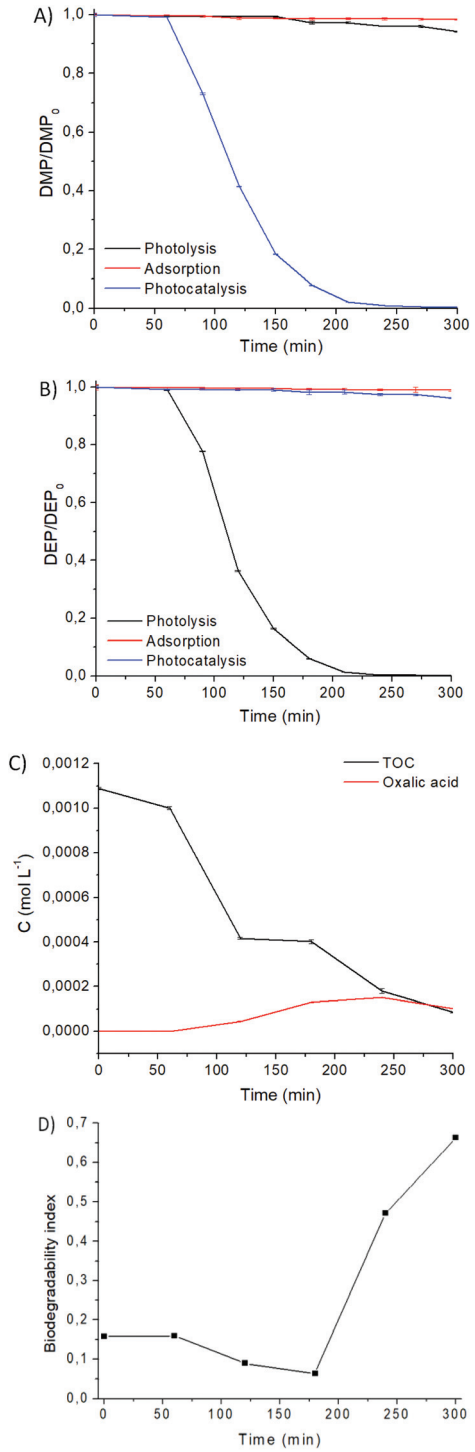

Fig. 3 Degradation of: (A) DMP and (B) DEP by heterogeneous photocatalysis; (C) content of organic carbon and generated oxalic acid; and (D) biodegradability index during degradation of DMP and DEP (initial concentration of DMP and DEP of 5 mg L^{-1} each, catalyst Degussa P25, dosage 1.5 g L^{-1} and dissolution pH = 10; n = 3 replicates for graphs (A), (B) and (C)).

A high mineralization percentage (≥70%) is related to smaller molecules such as carboxylic acids like oxalic acid, formic acid and acetic acid, as degradation products, less toxic than the initial PAEs.[22,33,46]

The biodegradability of organic matter is an important factor to know the capability to remove the organic matter under microbiological processes.[32] The biodegradability index (BOD_5/COD ratio) was calculated throughout the photocatalytic treatment (Fig. 3D). The results indicated that the sample before being treated had a biodegradability index of 0.16, which indicates that the effluent is not biodegradable. As the reaction time elapsed, a decrease in the biodegradability index was observed, reaching a value of 0.08 at 180 min, which indicates the formation of less biodegradable intermediates than DMP and DEP. However, the biodegradability index increased reaching a value of 0.66 after 300 min of reaction, which indicates that the sample is biodegradable. The results obtained from the analysis of BOD_5, COD and TOC, during the photocatalytic process demonstrated the efficiency of heterogeneous photocatalysis for the treatment of these types of emerging pollutants (DMP and DEP) producing a more biodegradable and less toxic effluent.

3.5. Identification of degradation intermediates and by-products

The intermediate products from DMP and DEP photocatalytic degradation were identified by GC-MS technique. A comparison with available standard compounds, instrumental library searches, and mass fragmentation patterns was carried out to identify degradation intermediates. The (a) DMP and (b) DEP photocatalytic degradation occurred through the oxidation initiated by $^{\bullet}OH$ radical attack resulting in the hydrolysis of the aliphatic chain and the hydroxylation of the aromatic ring (Fig. 4). Based on the identified transformation products, OH attack during photocatalytic treatment occurs mainly through the hydroxylation of the aromatic ring producing (c) dimethyl 4-hydroxyphthalate, (d) diethyl 4-hydroxyphthalate, (e) 5-hydroxy-2-(methoxycarbonyl) benzoic acid, (g) 2-(ethoxycarbonyl)-5-hydroxybenzoic acid, (i) 4-hydroxyphthalic acid, and (k) 2,4-dihydroxybenzoic acid intermediates. From the hydroxylation reaction, the main intermediates generated were (c) dimethyl 4-hydroxyphthalate and (d) diethyl 4-hydroxyphthalate, which are in concordance with the results reported by other authors.[46,47] The hydrolysis reaction of the aliphatic chain was also found to occur during the photocatalytic process. The intermediates formed were (f) 2-(methoxycarbonyl) benzoic acid, (h) 2-(ethoxycarbonyl) benzoic acid, (j) phthalic acid, and (l) phthalic anhydride. Obtaining (j) phthalic acid and (l) phthalic anhydride *via* hydrolysis was also reported by other authors.[22,39,46,47] Finally, the aromatic ring is opened, producing some carboxylic acids, such as (m) glutaric acid, (n) oxalic acid, and (o) acetic acid.

The presence of carboxylic acids was confirmed by IEC. A mixed standard stock solution containing carboxylic acids (acetic acid, formic acid, succinic acid, and oxalic acid) commonly described after the degradation of PAEs were injected into the IEC system to identify and quantify the short chain

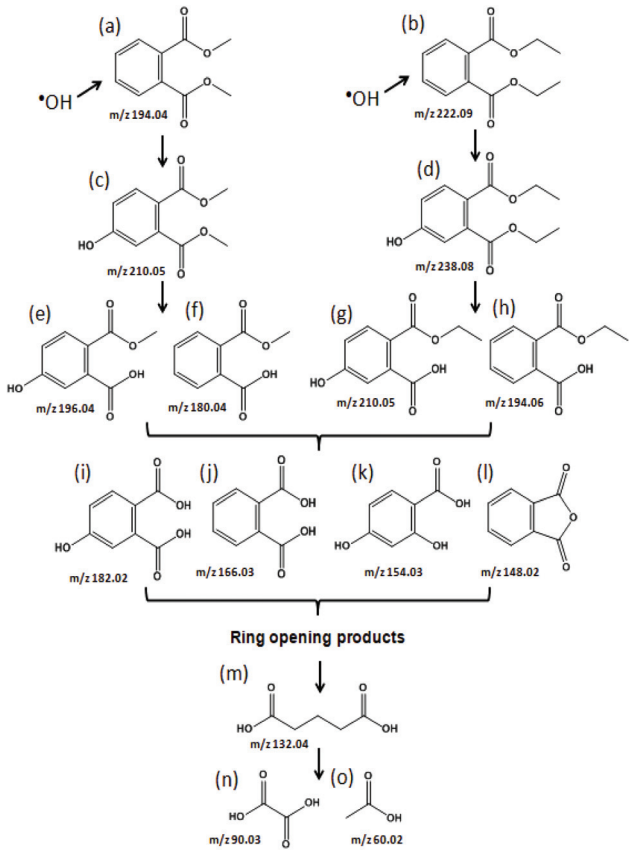

Fig. 4 Proposed degradation pathways of DMP and DEP with TiO_2 Degussa P25 (initial concentration of DMP and DEP of 5 mg L^{-1} each, catalyst dosage 1.5 g L^{-1} and dissolution pH = 10).

organic acids. However, due to the high detection limits of this technique and the low abundance of by-products generated, only oxalic acid was detected at a concentration of 4.6 mg L^{-1} after 300 min of reaction (Fig. 3C).

4. Conclusions

On-line monitoring of the photocatalytic degradation of DMP and DEP was automated by coupling the photoreactor to an HPLC system through an SIA system. This flow-based methodology enabled a real-time response of the degradation process with RSD values less than 1.6%. In accordance with the FFD, Degussa P25 showed the highest activity at a pH value and catalyst amount of 10 and 1.5 g L^{-1}, respectively. Under these experimental conditions, complete degradation and 92% mineralization were achieved after 300 min of reaction. Additionally, a drastic decrease in COD (from 49.1 O_2 L^{-1} initial to 3.8 mg O_2 L^{-1} after 300 min of reaction) allowed 92% removal. In the case of BOD_5, a decrease of 67% was observed, with an initial and final BOD_5 concentration of 7.7 mg O_2 L^{-1} and 2.5 mg O_2 L^{-1}, respectively. Hence, the photocatalytic treatment appears to be useful when there are easily biodegradable residues presenting a biodegradability index of 0.66 at the end of the reaction. During the photocatalytic reaction, not only did the hydrolysis reaction of the aliphatic chain occur, but also the hydroxylation of the aromatic ring, obtaining intermediates such as dimethyl 4-hydroxyphthalate, 4-hydroxy-diethyl phthalate, phthalic acid, and phthalic anhydride. However, after 300 min of reaction, the main by-products identified were carboxylic acids such as glutaric acid, oxalic acid and acetic acid.

Therefore, the efficiency of heterogeneous photocatalysis using TiO_2-based materials for the elimination of these highly toxic and recalcitrant emerging compounds was demonstrated.

Conflicts of interest

There are no conflicts to declare.

Acknowledgements

The authors are grateful for the financial support from the Facultad de Ciencias Químicas of the Universidad Autónoma de Nuevo León, the National Council of Science and Technology of México (CONACyT), the Spanish Ministerio de Economía y Competitividad (MINECO) and the European Funds for Regional Development (FEDER). D. Salazar-Beltrán acknowledges the University of Balearic Islands and CONACyT for scholarship support.

References

1 K. Khosravi and G. W. Price, *Microchem. J.*, 2015, **121**, 205–212.
2 M. J. Silva, A. R. Slakman, J. A. Reidy, J. L. Preau, A. R. Herbert, E. Samandar, L. L. Needham and A. M. Calafat, *J. Chromatogr. B*, 2004, **805**, 161–167.
3 W. J. Peijnenburg and J. Struijs, *Ecotoxicol. Environ. Saf.*, 2006, **63**, 204–215.
4 J. Yang, Y. Li, Y. Wang, J. Ruan, J. Zhang and C. Sun, *Trac, Trends Anal. Chem.*, 2015, **72**, 10–26.
5 M. Julinova and R. Slavik, *J. Environ. Manage.*, 2012, **94**, 13–24.
6 G. C. C. Yang, Y. H. Chiu and C. Wang, *Electrochim. Acta*, 2015, **181**, 217–227.
7 D. Salazar-Beltrán, L. Hinojosa-Reyes, E. Ruiz-Ruiz, A. Hernández-Ramírez and J. L. Guzmán-Mar, *Food Anal. Methods*, 2017, **11**, 48–61.
8 S. Net, A. Delmont, R. Sempere, A. Paluselli and B. Ouddane, *Sci. Total Environ.*, 2015, **515–516**, 162–180.
9 H. M. Zhao, H. Du, L. Xiang, Y. L. Chen, L. A. Lu, Y. W. Li, H. Li, Q. Y. Cai and C. H. Mo, *Environ. Pollut.*, 2015, **206**, 95–103.
10 P. Otero, S. K. Saha, S. Moane, J. Barron, G. Clancy and P. Murray, *J. Chromatogr. B*, 2015, **997**, 229–235.
11 U. Heudorf, V. Mersch-Sundermann and J. Angerer, *Int. J. Hyg. Environ. Health*, 2007, **210**, 623–634.
12 T. Fierens, K. Servaes, H. M. Van, L. Geerts, H. S. De, I. Sioen and G. Vanermen, *Food Chem. Toxicol.*, 2012, **50**, 2575–2583.

13 D. Gao, Z. Li, Z. Wen and N. Ren, *Chemosphere*, 2014, **95**, 24–32.
14 C. Pérez-Feás, M. C. Barciela-Alonso and P. Bermejo-Barrera, *Microchem. J.*, 2011, **99**, 108–113.
15 B. L. Yuan, X. Z. Li and N. Graham, *Water Res.*, 2008, **42**, 1413–1420.
16 D. Walter, L. Hsu-Chuen, C. Shu-Fei, T. K. Kuan and H. Chihpin, *J. Environ. Eng. Landsc.*, 2006, **16**, 275–282.
17 N. Adhoum and L. Monser, *Sep. Purif. Technol.*, 2004, **38**, 233–239.
18 F. Ma, S. Zhang, X. Yang, W. Guo, Y. Guo and M. Huo, *Catal. Commun.*, 2012, **24**, 75–79.
19 S. Anandan, N. Pugazhenthiran, T. Lana-Villarreal, G. Lee and J. J. Wu, *Chem. Eng. J.*, 2013, **231**, 182–189.
20 Y. Jing, L. Li, Q. Zhang, P. Lu, P. Liu and X. Lu, *J. Hazard. Mater.*, 2011, **189**, 40–47.
21 A. Haarstrick, O. M. Kut and E. Heinzle, *Environ. Sci. Technol.*, 1996, **30**, 817–824.
22 Y. H. Chen, L. L. Chen and N. C. Shang, *J. Hazard. Mater.*, 2009, **172**, 20–29.
23 M. Borges, D. García, T. Hernández, J. Ruiz-Morales and P. Esparza, *Catalysts*, 2015, **5**, 77–87.
24 D. C. Hurum, A. G. Agrios, K. A. Gray, T. Rajh and M. C. Thurnauer, *J. Phys. Chem. B*, 2003, **107**, 4545–4549.
25 H. Hou, M. Shang, L. Wang, W. Li, B. Tang and W. Yang, *Sci. Rep.*, 2015, **5**, 1–9.
26 G. Li, L. Chen, M. E. Graham and K. A. Gray, *J. Mol. Catal. A: Chem.*, 2007, **275**, 30–35.
27 A. Economou, *TrAC, Trends Anal. Chem.*, 2005, **24**, 416–425.
28 C. Chávez-Moreno, L. Ferrer, L. Hinojosa-Reyes, A. Hernández-Ramírez, V. Cerda and J. Guzmán-Mar, *J. Environ. Manage.*, 2013, **129**, 377–383.
29 E. Guevara-Almaraz, L. Hinojosa-Reyes, A. Caballero-Quintero, E. Ruiz-Ruiz, A. Hernández-Ramírez and J. L. Guzmán-Mar, *Chemosphere*, 2015, **121**, 68–75.
30 APHA, AWWA and WPCF, in *Métodos normalizados para el análisis de aguas potables y residuales*, ed. D. d. Santos, Madrid, España, 1992.
31 A. Asha, A. Muthukrishnaraj and N. Balasubramanian, *Int. J. Ind. Chem.*, 2014, **5**, 1–6.
32 K. Z. Abdalla and G. Hammam, *Int. J. Sci. Bas. Appl. Res.*, 2014, **13**, 42–48.
33 S. Kaneco, H. Katsumata, T. Suzuki and K. Ohta, *Chem. Eng. J.*, 2006, **125**, 59–66.
34 C. Karunakaran, D. Vasumathi and P. Vinayagamoorthy, *Indian J. Chem.*, 2015, **54A**, 1076–1084.
35 J. Yu, G. Wang, B. Cheng and M. Zhou, *Appl. Catal., B*, 2007, **69**, 171–180.
36 D. S. Kim, S. J. Han and S. Y. Kwak, *J. Colloid Interface Sci.*, 2007, **316**, 85–91.
37 R. López and R. Gómez, *J. Sol–Gel Sci. Technol.*, 2011, **61**, 1–7.
38 Z. Zhang, C. Wang, R. Zakaria and J. Y. Ying, *J. Phys. Chem. B*, 1998, **102**, 10871–10878.
39 M. Muneer, J. Theurich and D. Bahnemann, *J. Photochem. Photobiol., A*, 2001, **143**, 213–219.
40 M. N. Chong, B. Jin, C. W. Chow and C. Saint, *Water Res.*, 2010, **44**, 2997–3027.
41 D. Friedmann, C. Mendive and D. Bahnemann, *Appl. Catal., B*, 2010, **99**, 398–406.
42 J. M. Herrmann, *Top. Catal.*, 2005, **34**, 49–65.
43 X. R. Xu, S. X. Li, X. Y. Li, J. D. Gu, F. Chen, X. Z. Li and H. B. Li, *J. Hazard. Mater.*, 2009, **164**, 527–532.
44 B. Cagnon, S. Chatelain, T. Ferreira de Oliveira, F. Versaveau, S. Delpeux and O. Chedeville, *Water, Air, Soil Pollut.*, 2017, **228**, 1–10.
45 S. Ahmed, M. G. Rasul, R. Brown and M. A. Hashib, *J. Environ. Manage.*, 2011, **92**, 311–330.
46 B. L. Yuan, X. Z. Li and N. Graham, *Chemosphere*, 2008, **72**, 197–204.
47 Y. J. Jung, B. S. Oh, K. S. Kim, M. Koga, R. Shinohara and J. W. Kang, *J. Water Health*, 2010, **8**, 290–298.

